arXiv:1211.0694v1 [astro-ph.CO] 4 Nov 2012

Evolution of the First Supernovae in Protogalaxies: Dynamics of Mixing of Heavy Elements*

E. O. Vasiliev[1,2]†, E. I. Vorobyov[3], E. E. Matvienko,[2] A. O. Razoumov[4], Yu. A. Shchekinov[2]
[1]*Institute of Physics, Southern Federal University, Rostov-on-Don, Russia*
[2]*Physics Department, Southern Federal University, Rostov-on-Don, Russia*
[3]*Institute of Astronomy, University of Vienna, Austria*
[4]*SHARCNET/UOIT Consortium, Oshawa, Canada*

Abstract

The paper considers the evolution of the supernova envelopes produced by Population III stars with masses of $M_* \sim 25-200\ M_\odot$ located in non-rotating protogalaxies with masses of $M \sim 10^7\ M_\odot$ at redshifts $z = 12$, with dark-matter density profiles in the form of modified isothermal spheres. The supernova explosion occurs in the ionization zone formed by a single parent star. The properties of the distribution of heavy elements (metals) produced by the parent star are investigated, as well as the efficiency with which they are mixed with the primordial gas in the supernova envelope. In supernovae with high energies ($E \gtrsim 5 \times 10^{52}$ erg), an appreciable fraction of the gas can be ejected from the protogalaxy, but nearly all the heavy elements remain in the protogalaxy. In explosions with lower energies ($E \lesssim 3 \times 10^{52}$ erg), essentially no gas and heavy elements are lost from the protogalaxy: during the first one to threemillion years, the gas and heavy elements are actively carried from the central region of the protogalaxy ($r \sim 0.1\ r_{vir}$, where r_{vir} is the virial radius of the protogalaxy), but an appreciable fraction of the mass of metals subsequently returns when the hot cavity cools and the envelope collapses. Supernovae with high energies ($E \gtrsim 5 \times 10^{52}$ erg) are characterized by a very low efficiency of mixing of metals; their heavy elements are located in the small volume occupied by the disrupted envelope (in a volume comparable with that of the entire envelope), with most of the metals remaining inside the hot, rarified cavity of the envelope. At the same time, the efficiency of mixing of heavy elements in less energetic supernovae ($E \lesssim 3 \times 10^{52}$ erg) is appreciably higher. This comes about due to the disruption of the hot cavity during the collapse of the supernova envelope. However, even in this case, a clear spatial separation of regions enriched and not enriched in metals is visible. During the collapse of the supernova envelope, the metallicity of the gas is appreciably higher in the central region ($[Z] \sim -1$ to 0) than at the periphery ($[Z] \sim -2$ to -4) of the protogalaxy; most of the enriched gas has metallicities $[Z] \sim -3.5$ to -2.5. The masses of enriched fragments of the supernova envelope remain appreciably lower than the Jeans mass, except in regions at the center of the protogalaxy upon which the surrounding enriched gas is efficiently accreted. Consequently, the birth of stars with metallicities close to those characteristic of present-day Galactic stars is very probable in the central region of the protogalaxy.

1 Introduction

The first stars in the Universe began to be born in protogalaxies with total masses $M \sim 10^7\ M_\odot$ at redshifts $z \sim 12$ [1, 2]. The initial mass function of these first stars was probably shifted toward more massive stars due to the low efficiency of cooling when $T \lesssim 100$ K and the

*This paper is published in Astronomy Reports, 2012, Vol. 56, No. 12, pp. 895.
†eugstar@mail.ru

low opacity of the primordial gas [3]. The masses of the first stars probably lay in the interval from tens to hundreds of solar masses [4], making their lifetimes very short – in all, several million years [5]. After the numerical computations of [6], it has often been suggested that only one star initially arose in low-mass protogalaxies, although a group of stars could form under some conditions [7-10].

The first stars exerted an appreciable influence on the ambient medium. First, ionizing photons emitted by the first stars formed ionization zones, substantially redistributing the gas in their vicinity [11-18]. Second, the first stars exploded as supernovae (SN) at the end of their lives, ejecting heavy elements (metals) produced in their centers during their lifetimes into the surrounding space [19-26]. The number of ionizing photons, SN energy, and mass of ejected heavy elements depend on the mass of the star [27, 29]. The energy of SN explosions of massive stars could be sufficient to disrupt a protogalaxy [30, 31] and eject a substantial quantity of metals into intergalactic space [20]. The explosion of multiple SN will facilitate the formation of such outflows [32, 33]. Gas that has been enriched in heavy elements could be accreted onto neighboring protogalaxies and, when a metallicity above a certain critical value has been obtained [34-37], stimulate the formation of stars with a mass function close to the current one [23, 38]. Since stars can be born in a medium with any metallicity, transition-population stars with extremely low metal contents could be born in enriched gas [39, 40]; such stars could carry information about the chemical composition of the products of nucleosynthesis in the first stars [41, 42]. Low-mass stars with extremely low iron abundances [Fe/H] ~ -5 have recently been discovered in the Galaxy [43-46], some of which have appreciably higher abundances of other elements, e.g., [O/Fe] ~ 2 [47, 48]. However, stars with extremely low abundances of all elements [X/H] ~ -5 to -4, are also encountered [49]. These latter may be considered transition-population stars, but the question of their origin remains open [42].

Generally speaking, the spatial distribution of heavy elements (mixing) depends substantially on the relative flows of gas containing metals. When numerous shocks are present, the regions containing enhanced metal contents will be disrupted, and the distribution of heavy elemetns becomes more uniform (total mixing) [50]. If these relative motions die out in themedium, themetals will end up being contained in compact islands, which are not subsequently disrupted (incomplete mixing) [51, 52]. It is obvious that the effect of incomplete mixing will be enhanced in a radiatively cooled medium [51]. The characteristic time for the expansion and cooling of the envelopes of the first supernovae is fairly short, comprising several million years. There are no other sources to support the relative motions of gas during the explosion of a single star, and the gas motions die down as a consequence of efficient cooling in the envelope. As a result, heavy elements that are initially concentrated in the SN ejecta are poorly mixed with the entrained gas of the envelope [53]. Incomplete mixing could lead to the possible birth of stars with metallicities close to, or even exceeding, modern values. Moreover, since the energy of the explosion and the mass of ejected heavy elements depends on the mass of the star, the efficiency of mixing in early galaxy will be different following explosions of stars with different masses. Of course, when a star cluster exists at the center of a protogalaxy, a series of SN explosions is possible, whose energy could support the relative gas motions for a more prolonged time and facilitate more efficient mixing of the metals. However, the low efficiency of fragmentation in the primordial gas is not favorable for the birth of groups of stars.

Other factors that could lead to an enhancement of mixing could include mergers with lower-mass protogalaxies and the accretion of intergalactic gas, leading to turbularization of the gas in protogalaxies. Indeed, in a heirarchical model for the formation of structure, large objects appear as a result of mergers of smaller objects [54-57]; therefore, mixing can occur as the mass of the galaxy grows, when mergers or tidal and accretion flows encompss a mass comparable to the total mass of the galaxy. At later stages in the growth of a galaxy mass due to mergers, it must be taken into account that mergers with low-mas objects will exert only a local effect.

However, on long time scales, the regions of mixing will cover virtually the entire galactic disk, under the action of mergers. Mergers with protogalaxies with comparable masses occur rarely.the characteristic time between such merger events turns out to be appreciably longer than the time scale for the expansion and cooling of the SN envelope. The time for the accretion of intergalactic gas after virialization of the protogalaxy and the formation of the first stars is probably also longer than the cooling time for the SN envelope, due to the depletion of accreting material after virialization [58]. We do not consider the role of mergers and accretion in mixing of metals in more detail here. In the current paper, we restrict our analysis to the evolution of envelopes formed by single supernovae and study the efficiency of mixing of metals. Our computations assumed a ΛCDM cosmological model: $(\Omega_0, \Omega_\Lambda, \Omega_m, \Omega_b, h) = (1.0,\ 0.76,\ 0.24,\ 0.041,\ 0.73)$; the relative concentation of deuterium was taken to be $n[\mathrm{D}]/n = 2.78 \times 10^{-5}$ [59].

2 A model of a protogalaxy and numerical methods

In this section, we provide a brief description of themain parameters of the model, numerical methods (described in more detail in [10, 18, 60]), and initial conditions.

2.1 Main Parameters

In the model considered, a protogalaxy consists of gas surrounded by a spherically symmetrical halo of dark matter. The dark-matter density profile has the form of a modified isothermal sphere:

$$\rho_h(r) = \frac{\rho_0}{1 + (r/r_0)^2}, \tag{1}$$

where r_0 and ρ_0 are the radius of the core and the central density, and the total (dark halo and gas) mass of the protogalaxy M_h is taken to be $10^7\ M_\odot$. For redshift $z = 12$, this corresponds to 3σ perturbations in a ΛCDM model having parameter values equal to those derived from the results of three years of observations of the cosmic microwave background (CMB) radiation with the WMAP satellite [59]. The virial radius of such a protogalaxy is $r_v = 520$ pc (see the virial relations, for example, in [61]). It follows from simple estimates [1, 2] that a protogalaxy with a mass of $10^7\ M_\odot$ at redshift $z = 12$ is efficiently cooled, giving rise to the conditions required for the birth of the first generation of stars.

Since the minimum temperature of the primordial gas at high redshifts varies from 40 to 200 K, which facilitates the efficient formation of H_2 and HD molecules [2], the rate of accretion onto the protostellar core is higher than for the modern chemical composition of the gas ($\dot{M} \sim c_s^3/G$ [62]). Therefore, first-generation stars were substantially more massive than stars of subsequent generations. It follows from numerical models that their masses could vary within wide limits, $\sim 10 - 10^3\ M_\odot$ (see, e.g., [61]). We studied the evolution of the ionization zones surrounding stars with masses of 25, 40, 120, and 200 $M_\odot$ in [18]. This choice of masses was dictated by the fact that such stars explode as supernovae, ejecting the products of stellar nucleosynthesis into the surrounding gas, rather than collapsing directly into black holes [27].

The explosions of the first SN enriched the surrounding primordial gas in heavy elements (metals). The energy of the explosion and mass of metals produced during the lifetime of the star depends on the stars initial mass (Table). The presence of metals in the gas and their relative concentration determines the efficiency of star formation and the parameters of the stars that are born. Therefore, the redistribution of metals after the SN explosion is of fundamental importance for our understanding of the entire subsequent history of the evolution of the galaxy and its stellar populations. We present here computations for several models, whose parameters are presented in the Table. Note that the evolution of a star with a mass of 25 $M_\odot$ could proceed along at least two paths, and eject $\sim 2.1 M_\odot$ or $\sim 3.3 M_\odot$ of metals (models 25 and 25F in [63],

respectively). The explosion energy for massive stars (140-260$M_\odot$) is often assumed to be the same and equal to 10^{53} erg, although it was shown in [27] that this energy grows with mass from $\sim 10^{52}$ to 10^{53} erg. Since there are no data on the number of photons emitted by a star with a mass of 140 $M_\odot$ in [5], we used the data for a star with a mass of 120 $M_\odot$ to obtain the distribution of the gas before a SN explosion of a star with this mass.

Table 1: Main characteristics of the first supernovae

Stellar mass, $M_\odot$	Ejecta, $M_\odot$	Mass of metals, $M_\odot$	Explosion energy, erg	Refs
25	~ 21	~ 2.1	10^{51}	[63]
25	~ 22	~ 3.3	10^{52}	–
40	~ 34	~ 8.2	3×10^{52}	–
140	~ 140	~ 63	10^{52}	[27]
200	~ 200	~ 98.5	5×10^{52}	–

2.2 Numerical Scheme

The gas-dynamical equations were solved numerically in cylindrical coordinates under the approximation of axial symmetry (z, r, ϕ) using a finitedifference method with separation of operators [64]. A piecewise, parabolic, third-order interpolation scheme was used to transport the gas [65].

To obtain the initial distribution of the gas density in the external gravitational potential Φ_h of the dark matter, the equilibrium equation was solved numerically in cylindrical coordinates, (z, r). The gas was assumed to be neutral, to have a molecular weight $\mu = 1.22$, and to be isothermal, with a temperature equal to the virial temperature $T_{\rm vir}(M)$. Themethod used to solve the equilibrium equations is described in [66]. The interations were continued until the gasdensity profile corresponded to the mass of the gas inside the virial radius, $M_{\rm g} = (\Omega_b/\Omega_m)M_{\rm h}$. In our current study, we restrict our consideration to the evolution of spherical (non-rotating) protogalaxies.

It is assumed in our model that all chemical reactants (atoms, ions, molecules) move like passive components; i.e., they have the same velocity field as the gas, making it possible to restrict our solution to the equations of motion of the gas. The chemical kinetics of the primordial gas include the following main components: H, H^+, H^-, He, He^+, He^{++}, H_2, H_2^+, D, D^+ and HD. To compute the electron concentration, we assumed conservation of charge. The mass fraction of helium was taken to be $Y_{\rm He} = 0.24$.

We considered two temperature intervals in our chemical-kinetics computations: high-temperature ($T > 2 \times 10^4$ K) and low-temperature ($T < 2 \times 10^4$ K). At the high temperatures, the concentrations of ions and molecules were calculated from their equilibrium values, while a system of equations for the non-equilibrium chemical kinetics was solved in the low-temperature case. The rates of chemical reactions were taken from [67-69]. The chemical kinetics equations were solved using a fifth-order RungeKuttaCusp method with automatic step selection [70].

The energy equation took into account radiative losses characteristic of the primordial gas: cooling during recombination, collisional excitation of hydrogen and helium, freefree transitions, Compton interactions with CMB photons [71], and molecular cooling of H_2 [69] and HD [72, 73]. The contribution of metals should also be included for gas with non-zero metallicity. The cooling function in the high-temperature region was calculated for a collisional gas with a metallicity of $(0.001 - 4)\ Z_\odot$ using the method of [74] and is presented as a table of $\Lambda(T, Z)$ values (about 20 metallicities and about 100 temperatures). In the low-temperature region, it was assumed that metals contributed to cooling via energy losses in fine-structure lines of carbon and oxygen

[36]. The kinetics of these elements was not calculated separately, and it was assumed that all the carbon was singly ionized and that the oxygen was neutral, which is fully acceptable for the conditions considered [36]. Moreover, we included the effect of interactions between molecules, ions, and atoms of metals with CMB photons [75-77]: when gas temperatures close to the CMB temperature are reached, molecules, ions, and atoms of metals can be excited by CMB photons, and may transfer energy to the gas during collisions, heating this gas.

2.3 Initial Conditions

In our computations, we assumed that the dark matter in a protogalaxy at redshift $z = 12$ is already virialized, so that it has achieved a configuration described by (1). The protogalaxy gas cools, and the gas concentration in the central region grows, reaching $\sim 10^8$ cm^{-3} in our computations. Further, we assume that a star is born in the center of the protogalaxy.

The ionizing photons from the star form a surrounding ionization zone, which encompasses an appreciable volume in the protogalaxy by the end of the stars lifetime [18]. As initial conditions before the SN explosion, we took the distributions of the density, temperature, and chemical components obtained in our computations [18] at the end of the lifetime of a star with the corresponding mass. A thermal energy corresponding to the explosion energy and a mass of metals are added to a central region with a radius of two parsec (Table).

We used a non-uniform computational grid to improve the resolution at the center of the protogalaxy [10]. The density of the grid can be controlled using a coefficient A: decreasing A leads to an increase in resolution in the inner regions of the computational grid and a decrease in resolution in outer regions. In our computations, we adopted $A = 1.5$ and used a 900×900 grid, which corresponds to a physical resolution better than 0.1 pc in a region with a radius of 10 pc, which degrades to ~ 1 pc at a radius of $r \simeq 200$ pc. The inhomogeneous division of the grid was the same in the z and r directions.

3 Evolution of gas and metallicity

In a high-energy SN explosion ($E \sim 10^{53}$ erg) in a protogalaxy with mass $M \lesssim 10^7 M_\odot$, the kinetic energy of the expanding gas envelope is sufficient for it to reach the virial radius of the protogalaxy, so that the protogalaxy is essentially disrupted [30, 31]. The gas in such objects will be essentially fully swept out by the SN explosion, and the protogalaxy will be filled with the hot ($T \sim 10^5 - 10^6$ K), rarified ($n \sim 10^{-4} - 10^{-3}$ cm^{-3}), very high-metallicity gas ejected by the SN, which occupies a volume corresponding to more than half the virial radius of a protogalaxy with mass $M \sim 10^7\ M_\odot$. The metallicity of this gas is determined by the mass of the star, and can exceed the solar value by more than an order of magnitude – practically half the mass of the SN can be reprocessed into heavy elements [27]. The cooling time in the hot gas, which is of the order of several million years, turns out to be comparable to or longer than the time scale for the loss of an appreciable mass of gas (about 50%), since the remaining gas is located at the periphery of the galaxy (at distances exceeding the virial radius), and its velocities are comparable to the escape speed [60] (see also our figure for the SN model with $M = 200\ M_\odot$ and $E = 5 \times 10^{52}$ erg). Such dark (with a low mass of gas) dark-matter halos will merge with lowermass, gas-rich protogalaxies in which star formation has not occurred, and in which a sufficient mass of gas for star formation may accumulate in the future. Note also that such dark halos could be invisible satellites of galaxies: there appears to be a discrepancy between the numbers of theoretical and observed satellites in the Galaxy - the so-called missing-satellites problem [78]. Another consequence of a high-energy SN explosion in a low-mass halo could be modification of the dark-matter profile in the protogalaxy, such as a transition from a cusp to a flat profile [79-81].

The masses of the first stars could vary within fairly broad limits, from several tens to several hundreds of solar masses (see, e.g., [61]). Of course, the energy of the SN depends on the mass of the star and varies in the range $E \sim 10^{51} - 10^{53}$ erg [27]. Consequently, the kinetic energy of the gas in the SN remnant may be insufficient to overcome the gravitation of the dark halo of the protogalaxy, so that all (or a large fraction of) the gas remains inside the protogalaxy. The hot cavity[1] gradually cools, the pressure is lowered, and part of the gas in the SN envelope begins to move toward the center of the protogalaxy due to the gravitational field of the dark halo; i.e., the collapse of the SN envelope begins. It is natural to expect that the primordial, or metal-poor, gas in the envelope mixes with the metal-rich gas of the ejecta.

Figures 1 and 2 show the distributions of the density and temperature of the gas, the relative concentration of molecular hydrogen, and the metallicity at times t = 1, 5, 10, 15, 20 Myr (from top to bottom) after the explosion of a SN with an initial mass of 140 $M_\odot$ and an energy of 10^{52} erg in the center of a spherical protogalaxy with a total mass of $M = 10^7$ $M_\odot$. The SN envelope has formed by time $t = 1$ Myr, when it almost reaches a radius of 100 pc, which corresponds to about one-fifth of the virial radius. Small perturbations of the density in the envelope due to the Rayleigh-Taylor instability can be seen. These perturbations lead to fragmentation and the almost total disruption of the envelope, as is visible in the lower maps in Fig. 1. Since the gas in the envelope cools efficiently, thermal instability also plays a role in the fragmentation of the gas. Extended tongues with lower density and higher temperature had already formed during the existence of the parent star, due to penetration of the ionization zone [18]. Due to the enhanced degree of ionization, molecular hydrogen forms efficiently in the SN envelope and remnant HII zone, which cools the gas when $T \lesssim 10^4$. However, this is not the only source of cooling of the gas in the SN envelope. A small fraction of the heavy elements of the ejecta gradually become mixed with the primordial, swept up gas at the inner side of the envelope. We can clearly see that the efficiency of the mixing is low, since all the heavy elements are contained in the hot cavity (upper maps in Fig. 1). At later times, heavy elements can be seen in disrupted fragments of the envelope (subsequent maps of Fig. 1).

As was indicated above, with time, the pressure of the hot gas in the cavity is reduced by cooling, and the SN envelope begins to collapse under the action of the gravitation of the dark halo; this is visible in Fig. 1 for $t = 5$ Myr (third row of maps from the top). This is more clearly visible for the subsequent time $t = 10$ Myr. Some envelope fragments continue to move away from the center, but part of the envelope moves toward the center, gradually mixing with the hot, metal-rich gas in the cavity. We can clearly see that H_2 (Fig. 2), and then HD, molecules form efficiently in the envelope fragments, the gas cools rapidly, and the temperature falls below 100 K in some regions (Fig. 1). The gas flows converging on the central region of the protogalaxy form a series of shocks and near-acoustic waves, which facilitate mixing of the hot, high-metallicity gas of the cavity with the cool, primordial (low-metallicity) gas of the envelope fragments. By time $t = 20$ Myr (lower maps in Figs. 1, 2), a gravitational-compression regime is established in the central region of the protogalaxy, and the gas density reaches $n \sim 10^6$ cm^{-3}; we ceased the computations at this point, since our model does not include physical processes that can occur in such a dense, metal-rich gas (the formation of CO and OH, and the loss of energy via lines of these molecules). It is obvious that the conditions required for star formation will arise in this region. This possibility will be discussed below.

Comparing the density and metallicity distributions of the gas that have been established by a time $t = 20$ Myr (lower maps in Figs. 1, 2), we note that heavy elements are essentially strictly localized in fragments of the disrupted envelope, although the gas in some of these is still

[1] We will understand the cavity to be the region containing the hot gas in the central region of the protogalaxy, which contains part of the unmixed ejecta). The ejecta is the heavy-element-enriched gas ejected from the parent star. Subsequently, the accumulated primordial gas in the SN envelope mixes with the highly enriched gas, and so will contain part of the ejecta.

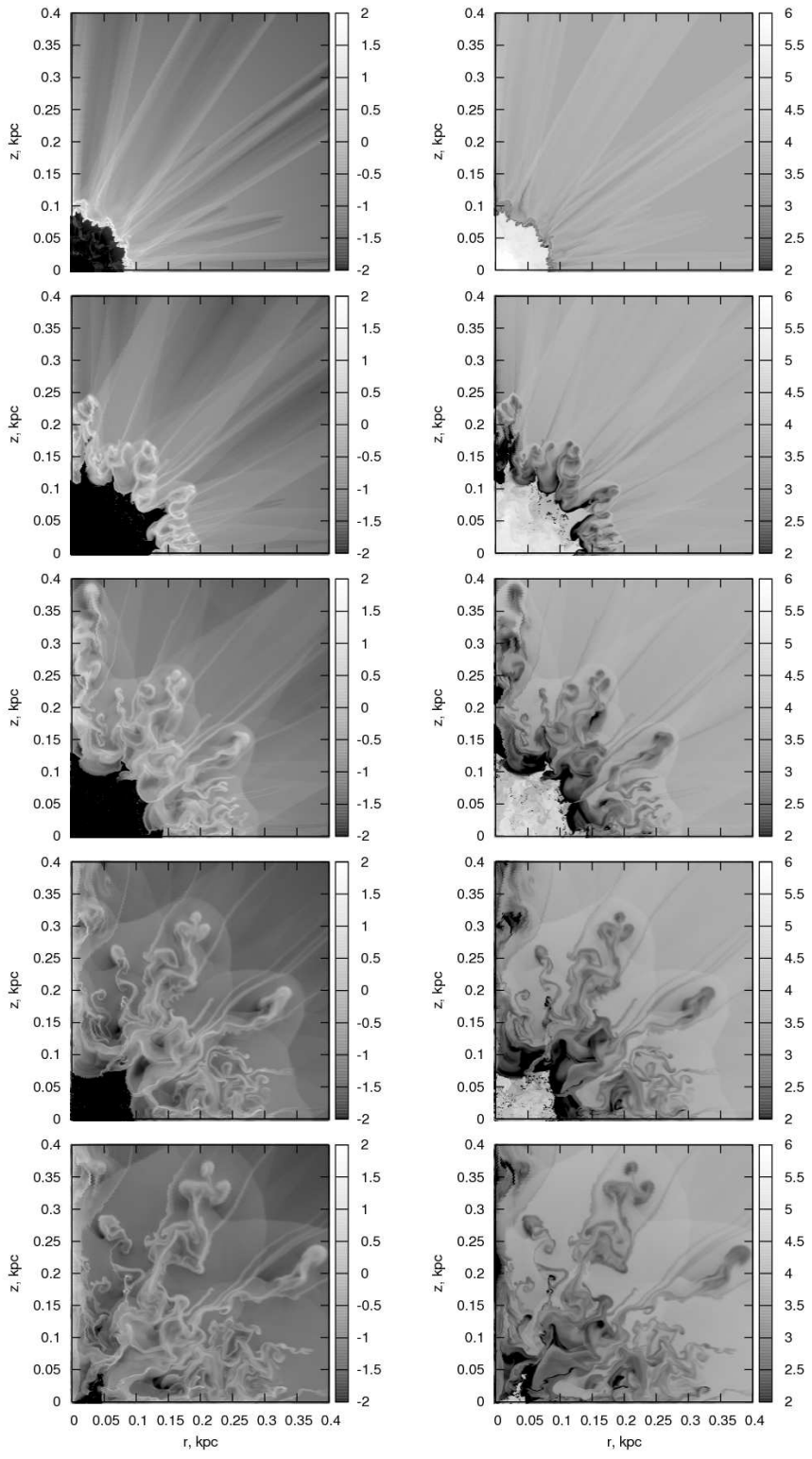

Figure 1: Distribution of the density (left) and temperature (right) of the gas at times $t = 1, 5, 10, 15, 20$ Myr after the explosion of a star with mass 140 $M_\odot$ and energy 10^{52} erg (from top to bottom) in the central region of a protogalaxy with a total mass $M = 10^7$ $M_\odot$.

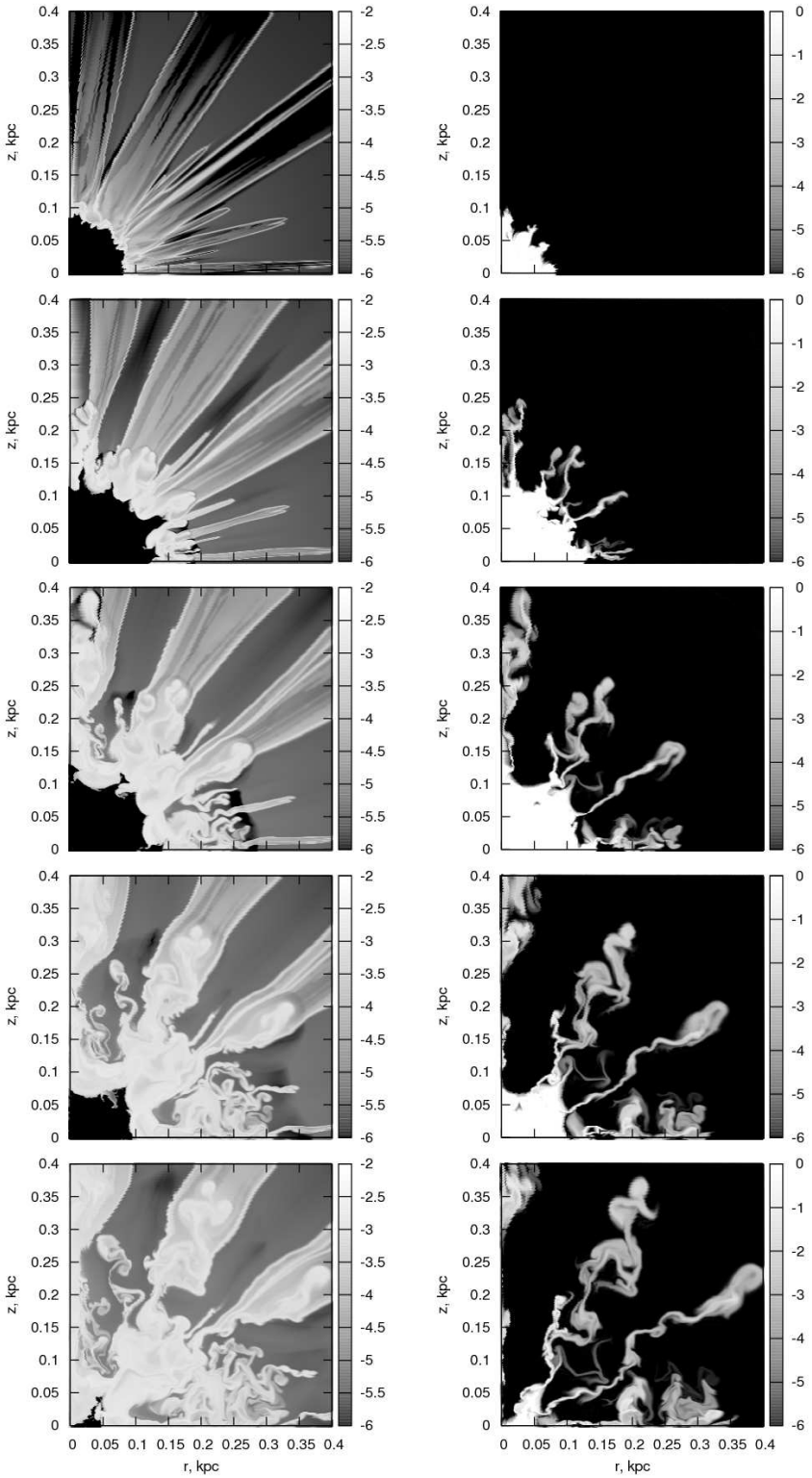

Figure 2: Same as Fig. 1 for the relative concentration of molecular hydrogen (left) and the metallicity (right) of the gas.

primordial. Moreover, heavy elements are visible in thread-like structures, which formed when the fragments became distinct as a result of RayleighTaylor instability. This is a consequence of the fact that some of the highly enriched gas of the ejecta is entrained into fragments during their formation. The metallicities of the gas in the fragments and these thread-like structures are comparable, $[Z] \simeq -4$ to -2. An appreciable fraction of the heavy elements is concentrated in the central region, where the metallicity of the gas can reach $[Z] \simeq -1$ to 0. Overall, however, the mixing is incomplete, as is manifest by the extremely nonuniform distribution of heavy elements: fairly enriched regions ($[Z] \simeq -3$) and regions of primordial gas can be located virtually right next to each other.

Overall, the evolution of the SN remnant for other explosion energies for which there is a collapse of the hot cavity resembles the picture described above. Differences are associated primarily with the initial conditions in the protogalaxy before the explosion, i.e., the gas distribution established in the ionization zone by the end of the stars lifetime and the properties of the SN – the mass of heavy elements ejected during the explosion and the explosion energy. All this influences the size of the region containing heavy elements, and therefore the efficiency of mixing of the heavy elements. For comparison, we present the gas density and metallicity distributions at the times when the conditions for the formation of the next generation of stars have arisen (a gravitational contraction regime has been established in the central region of the protogalaxy, the gas density reaches $n \sim 10^6$ cm^{-3}).

Figure 3 shows the distributions of the gas density (left) and metallicity (right) after the explosions of supernovae with masses and energies $M = 25\ M_\odot$ and $E = 10^{51}$ erg, $M = 25\ M_\odot$ and $E = 10^{52}$ erg, $M = 40\ M_\odot$ and $E = 3 \times 10^{52}$ erg, $M = 140\ M_\odot$ and $E = 10^{52}$ erg, $M = 200\ M_\odot$ and $E = 5 \times 10^{52}$ erg (from top to bottom) at times $t = 4.4, 13, 20, 20$, and 16 Myr, respectively. The distributions for the SN with high energy ($M = 200\ M_\odot$ and $E = 5 \times 10^{52}$ erg; lower panels) are shown for late times, when an appreciable fraction of the gas of the protogalaxy has crossed the virial radius. Note that the scales along the y axes for the various distributions shown in Fig. 3 are different. The character of the distribution of heavy elements is the same for all the collapsed SN envelopes: the heavy elements are poorly mixed, and contained within strictly localized structures. For all the models considered, the metallicities in these structures lie in the range $[Z] \simeq -4$ to -2.

The volume of gas encompassed by the shock increases. Shortly thereafter, the volume of the enriched gas likewise grows, as is clearly visible in Fig. 3. The same is true for the mass of the enriched gas. As an example, Figure 4 (two upper panels) shows the evolution of the mass and volume of the gas with metallicity above a specified level inside the virial radius following a SN explosion with initial mass 140 $M_\odot$ and energy 10^{52} erg. The mass of enriched gas ($[Z] > -5$) grows with time, approaching saturation at times $t \gtrsim 15$ Myr. The mass and volume of gas with metallicity $[Z] > -2$ saturates by $t \sim 7 - 8$ Myr. This indicates weak mixing of this gas at subsequent times. This gas should remain in the central region of the protogalaxy, and the enrichment of the expanding fragments virtually ceases. The gas in these fragments is not enriched above a metallicity $[Z] \sim -2$. Note that the mass of high-metallicity gas ($[Z] > 0$) remains constant with time. The volume occupied by this gas grows over the first five million years, then decreases. This corresponds to the initial expansion and subsequent compression of the hot cavity. Note here that a SN envelope with high energy ($E \sim 5 \times 10^{52} - 10^{53}$ erg) encompasses virtually the whole of a protogalaxy with mass $10^7\ M_\odot$, but the heavy elements remain concentrated in the rarified, highly enriched cavity (lower panels in Fig. 3). A substantial fraction of the heavy elements in collapsing envelopes is associated with dense, i.e., fairly cool (Figs. 1, 2), gas.

Figure 4 also shows (two lower panels) the evolution of the mass and volume of the gas in metallicity intervals inside the virial radius following the explosion of a SN with initial mass 140 $M_\odot$ and energy 10^{52} erg. The gas with intermediate metallicities, $-3.5 < [Z] < -2$, has the

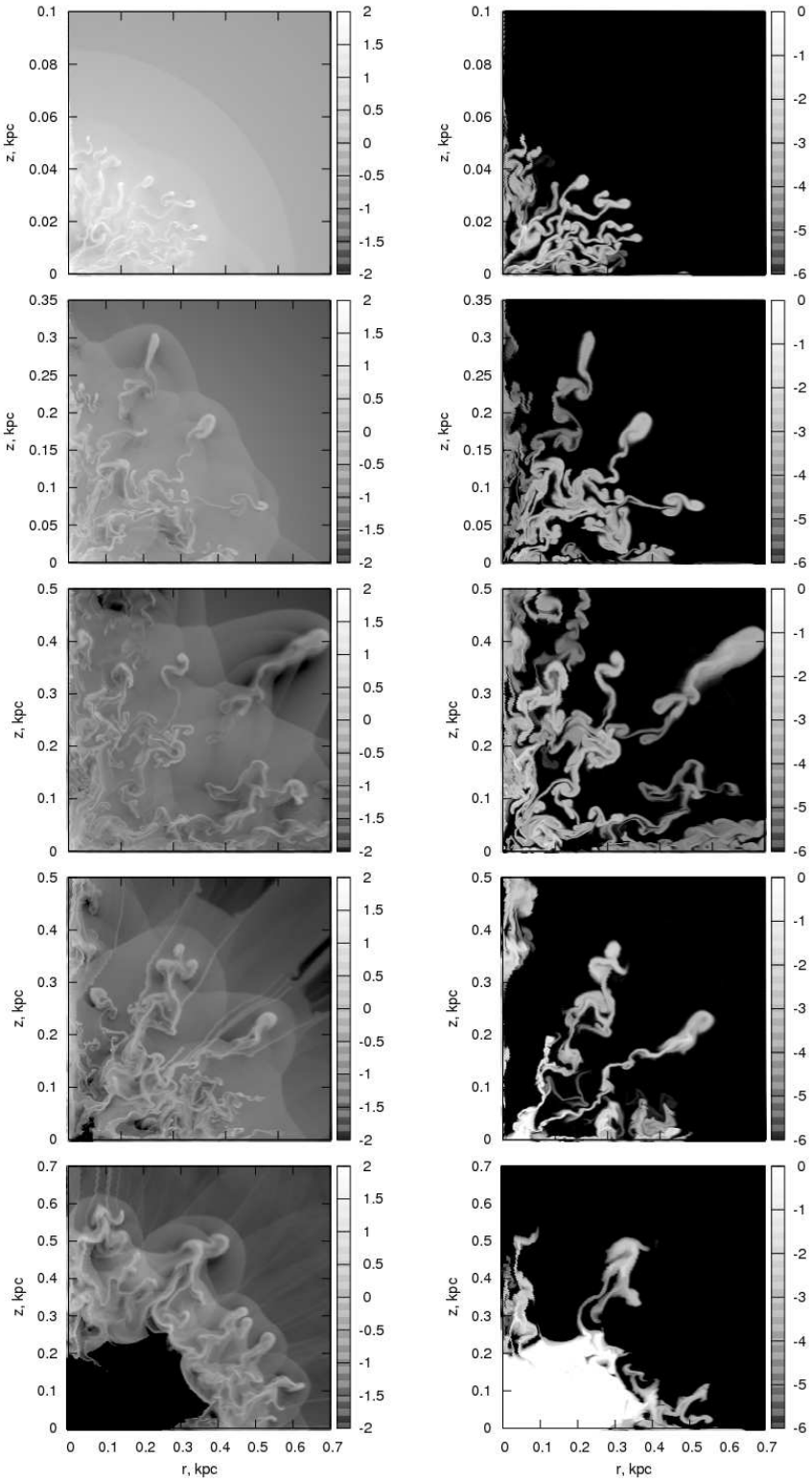

Figure 3: Distributions of the density (left) and metallicity (right) of the gas at the final times following SN explosions in a protogalaxy with total mass $M = 10^7\ M_\odot$ (from top to bottom): $t = 4.4$ Myr for a star with mass 25 $M_\odot$ and a SN energy 10^{51} erg, $t = 13$ Myr for a star with mass 25 $M_\odot$ and a SN energy 10^{52} erg, $t = 20$ Myr for a star with mass 40 $M_\odot$ and a SN energy 3×10^{52} erg, $t = 20$ Myr for a star with mass 140 $M_\odot$ and a SN energy 10^{52} erg, $t = 16$ Myr for a star with mass 200 $M_\odot$ and a SN energy 5×10^{52} erg.

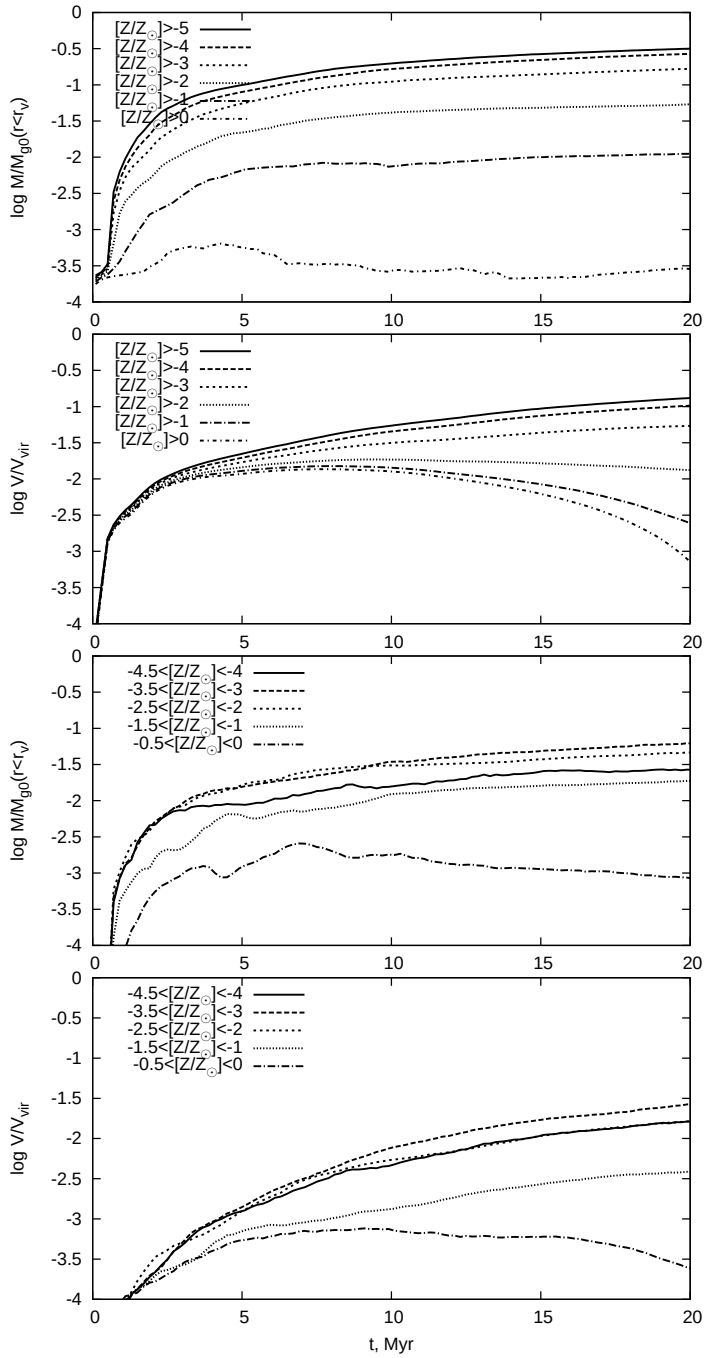

Figure 4: Evolution of the mass and volume of the gas with metallicity above a specified level (upper panels) and in intervals (lower panels) inside the virial radius following an explosion of a star with mass 140 $M_\odot$ and an SN energy of 10^{52} erg.

greatest mass and volume, although the number of cells with such metallicities is not large (see the following section). This gas is primarily concentrated in fragments of the envelope at large distances from the center. Here, we must bear in mind that our computations were carried out in a cylindrical geometry; i.e., the cells at the periphery have substantially larger volumes than those in the central region of the protogalaxy.

As was noted above, the volume and mass of the enriched gas depend on the SN energy, and some of the gas can leave the protogalaxy. Figure 5 presents the evolution of the mass of gas and heavy elements ejected beyond radii of 0.05 r_v, 0.1 r_v, and 1.0 r_v during the explosion of a SN with energy E and initial mass M. An appreciable fraction of the gas is ejected from the galaxy only for the SN with energy $E = 5 \times 10^{52}$ erg and mass $M = 200\ M_\odot$ (lower panels). Roughly one-third of the mass of gas has passed beyond the virial radius by time $t = 20$ Myr. The loss of metals is smaller, comprising about one-tenth of the mass of heavy elements. The remaining metals are located primarily in the hot cavity. The cooling time of the hot gas, which is approximately several million years, is longer than the time scale for the loss of an appreciable fraction of the gas mass (more than 50%), since the mean velocity of the gas at the periphery of the galaxy (at radii exceeding half the virial radius) is comparable to the escape velocity for the protogalaxy considered. Thus, a protogalaxy with mass $M \sim 10^7\ M_\odot$ in which high-energy supernovae explode with with high probability become a "dark" object with essentially no gas.

The explosion of a SN with energy $E = 3 \times 10^{52}$ erg and initial mass $M = 40\ M_\odot$ (third row of panels from the top) is accompanied by a more modest loss of gas (up to one-tenth of the mass of gas). The mass of gas within radii of 0.05 r_v and 0.1 r_v falls sharply following the explosion, decreasing by several orders of magnitude in the first 1.5 Myr after the explosion. The mass of metals behaves similarly. However, beginning from 8 Myr, the gas begins to return to the central region of the protogalaxy - the SN envelope begins to collapse. By 20 Myr, the mass of gas at distances $r < 0.05 r_v$ has actually increased by an order of magnitude, compared to its value before the explosion. An appreciable fraction of the mass of metals (about 50%) is concentrated within $r < 0.05 r_v$.

The loss of gas and metals from the protogalaxy is insigificant for the remaining three models ($M = 25\ M_\odot$ and $E = 10^{51}$ erg, $M = 25\ M_\odot$ and $E = 10^{52}$ erg, $M = 140\ M_\odot$ and $E = 10^{52}$ erg) (see the corresponding panels in Fig. 5). The evolution of the mass of gas and metals in the model with $M = 140\ M_\odot$ and $E = 10^{52}$ erg resembles the evolution described for $M = 40\ M_\odot$ and $E = 3 \times 10^{52}$ erg, and we do not considered it in detail here. The redistribution of gas and metals for a SN with $M = 25\ M_\odot$ occurs within 0.05 r_v and 0.1 r_v for SN energies $E = 10^{51}$ erg and $E = 10^{52}$ erg, respectively; up to 90%, and for $E = 10^{51}$ erg up to 99%, of the mass of metals is retained within the region $r < 0.1\ r_v$.

Heavy elements facilitate more efficient cooling of the gas than do H_2 and HD molecules [34]. The first stars emit a substantial number of photons at $11 - 13.6$ eV [5], which are capable of disrupting H_2 molecules if their column density is small, so that self-shielding is not important. Therefore, the relative number density of H_2 in the surrounding medium is fairly low by the end of the star's lifetime in most of the models considered: $\sim 10^{-6}$. The gas density in the unstable envelope formed by the ionization front increases and the temperature decreaes with decreasing mass of the star and decreasing number of ionizing photons [18]. The source of ionizing radiation "switches off" by the time of the SN explosion, and conditions favorable for the formation of molecular hydrogen arise in the ionized gas of the envelope. Therefore, the SN shock front propagates through gas in whichmolecules are already efficiently forming.

Figure 6 depicts the evolution of the masses of gas with relative number densities of H_2 exeeding 5×10^{-4} and 10^{-3}, and also with temperatures below 100, 200, and 1000 K, inside the virial radius r_v for a SN explosion with energy E and initial mass M. Due to the high gas density in the envelope of the ionization zone, the mass of H_2 grows rapidly in the model with $M = 25\ M_\odot$: the relative number density has reached $\sim 10^{-3}$ in the densest fragments of the

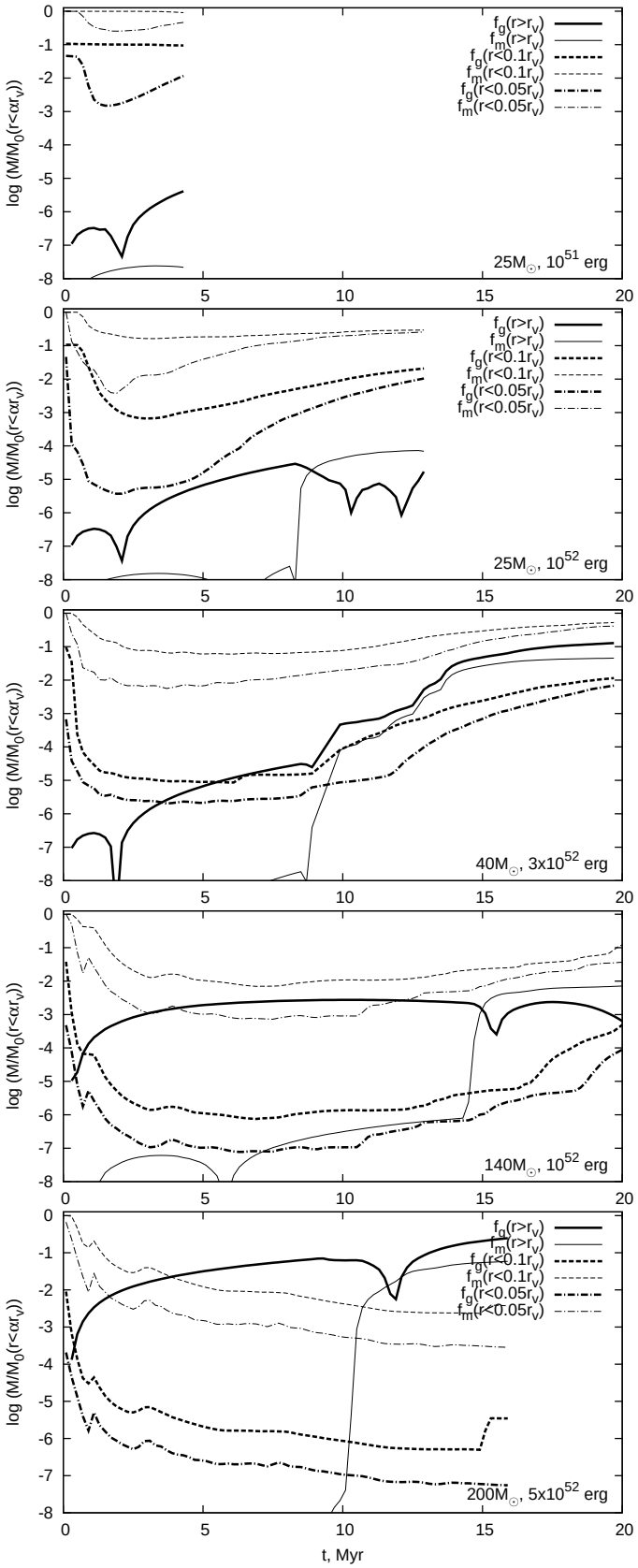

Figure 5: Mass fraction of gas f_g and heavy elements f_m remaining in the halo and ejected from the halo during a SN explosion with energy E and initial mass M. M_0 is the mass of gas (metals) outside or inside the radius αr_v ($\alpha = 0.05, 0.1, 1$) at the moment of the SN explosion.

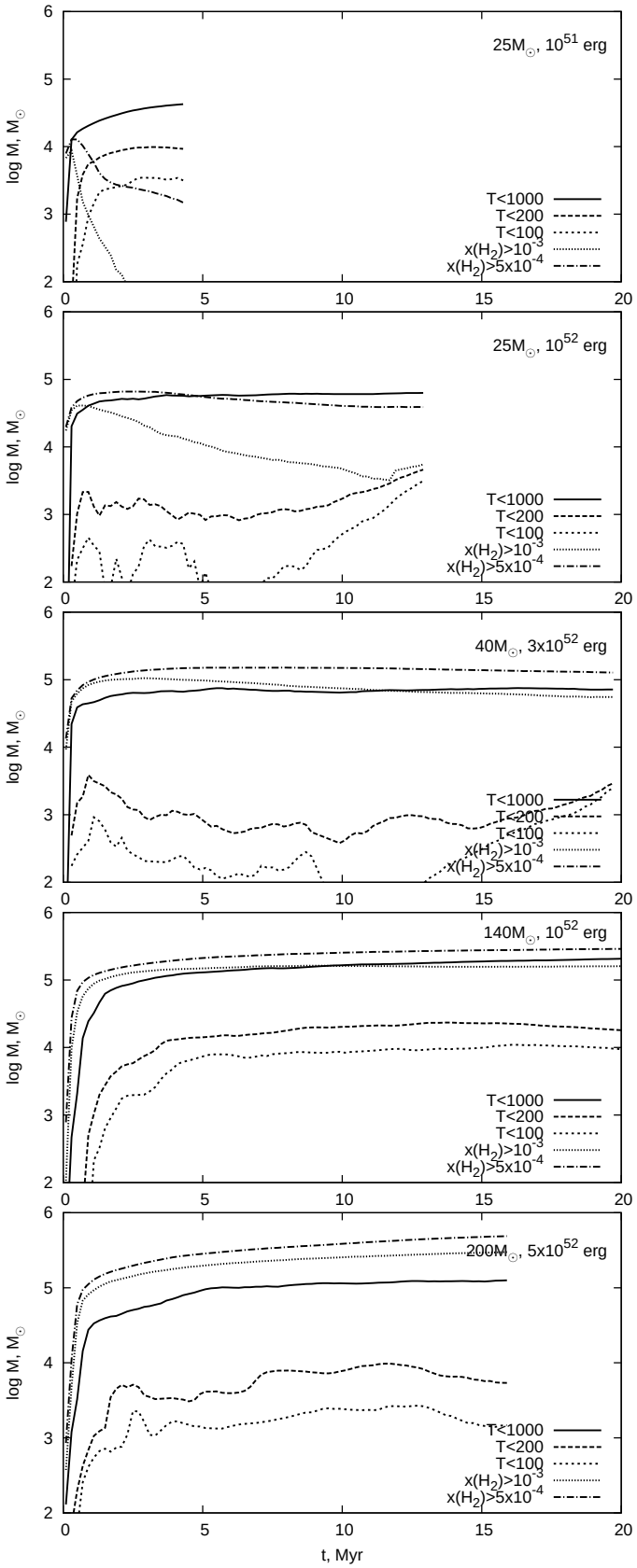

Figure 6: Evolution of the mass of gas with relative number densities of H_2 exceeding 5×10^{-4} and 10^{-3}, and also with temperatures below 100, 200, and 1000 K, within the virial radius r_v for a SN explosion with energy E and initial mass M.

envelope essentially after $0.1 - 0.2$ Myr. The SN shock rapidly propagates in the hot remnant of the ionization zone, disrupting the molecules formed there; in the case $M = 25\ M_\odot$ (two upper panels in Fig. 6), the mass of gas with number densities higher than 10^{-3} falls rapidly. As the SN envelope expands, the gas in the envelope cools, so that molecular hydrogen again begins to form. Accordingly, the mass of gas with molecular hydrogen number densities above 5×10^{-4} for a SN with energy $E = 10^{51}$ erg displays a modest break at $t \sim 1.5$ Myr, and this gas mass decreases only slightly with time in the case of a SN with higher energy, $E = 10^{52}$ erg. In the remaining models, the mass of molecular gas grows due to the formation of molecules in the SN envelope and in weakly ionized "lobes" – remnants of the disrupted ionization-zone envelope [18], visible in Fig. 2 as diverging "rays" with higher molecular number densities.

In the model with $M = 25\ M_\odot$ and $E = 10^{51}$ erg (lower panels in Fig. 6), the mass of cool gas with temperatures below 100, 200, and 1000 K grows with time. Since the H_2 molecules are rapidly destroyed, the gas can be cooled only by energy losses in lines of heavy elements. Consequently, metals from the ejecta are mixed with gas in the SN envelope, leading to a drop in the temperature and the subsequent development of instability. This leads to the disruption and collapse of the envelope, and to more efficient mixing of heavy elements. As the explosion energy grows (second row of panels from the top of Fig. 6), the mass of gas with temperatures below 1000 K grows rapidly and saturates, but the gas is inefficiently cooled to lower temperatures, and the mass of cooler gas remains low. Note that the mass of gas with a relative number density of H_2 above 5.10.4 is roughly equal to the mass of gas with $T < 1000$ K; consequently, this suggests that the gas is cooled primarily by the H_2. Only after disruption of the envelope due to instability and the onset of the collapse of the cavity does the mass of gas with temperatures below 200 K, or even below 100 K, begin to increase. This is obviously related to mixing of the heavy elements, and therefore to more efficient cooling in lines of heavy elements. The case of a more massive SN with $M = 40\ M_\odot$ (third row of panels) resembles the previous case the model with $M = 25\ M_\odot$ and $E = 10^{52}$ erg. When the initial mass of the star becomes $M = 140\ M_\odot$, the formation of molecules is efficient not only in the strongly disrupted envelope, but also in the lobes (see above and Fig. 2), so that the mass of gas in regions with temperatures below 100, 200, and 1000 K grows. The behavior is similar for a SN explosionwith $M = 200\ M_\odot$. Thus, cooling of the gas below 100 K in a collapsing SN is brought about primarily by losses in lines of metals, which are mixed with the primordial gas during the disruption and subsequent collapse of the SN envelope.

4 Statistics of the distribution of gas and heavy elements

The heavy elements are initially concentrated in the gas ejected by the SN, whose metallicity is determined by the mass of metals produced in the star (Table). It is obvious that this metallicity will be fairly high: $\gtrsim 10\ Z_\odot$. After the SN explosion, the expanding envelope sweeps up the surrounding primordial gas (this gas had a metallicity $10^{-6}\ Z_\odot$ in our computations), and metals remain in the hot cavity. The SN envelope is disrupted by hydrodynamical instability, and the metals mix with the primordial gas. However, we can speak of mixing only when considering averaging over large scales. There are strictly localized islands of gas enriched in metals (Fig. 2), which correspond to the characteristic properties of systems with regions of intermittency – sharp spatial alternation of regions with high and low metallicity, with these values sometimes differing by an order of magnitude.

Figure 7 shows the distribution of the number of computation cells with various gas metallicities $N(Z)$ normalized to the total number of computation cells for a SN explosion with energy 10^{52} erg and initial mass 140 $M_\odot$ at times 1, 5, 10, 15, and 20 Myr. Peaks corresponding to gas in the cavity (high metallicity) and the unperturbed gas ahead of the shock front ($Z = 10^{-6}\ Z_\odot$) are clearly visible. With time, the number of cells with intermediate metallicities grows, but

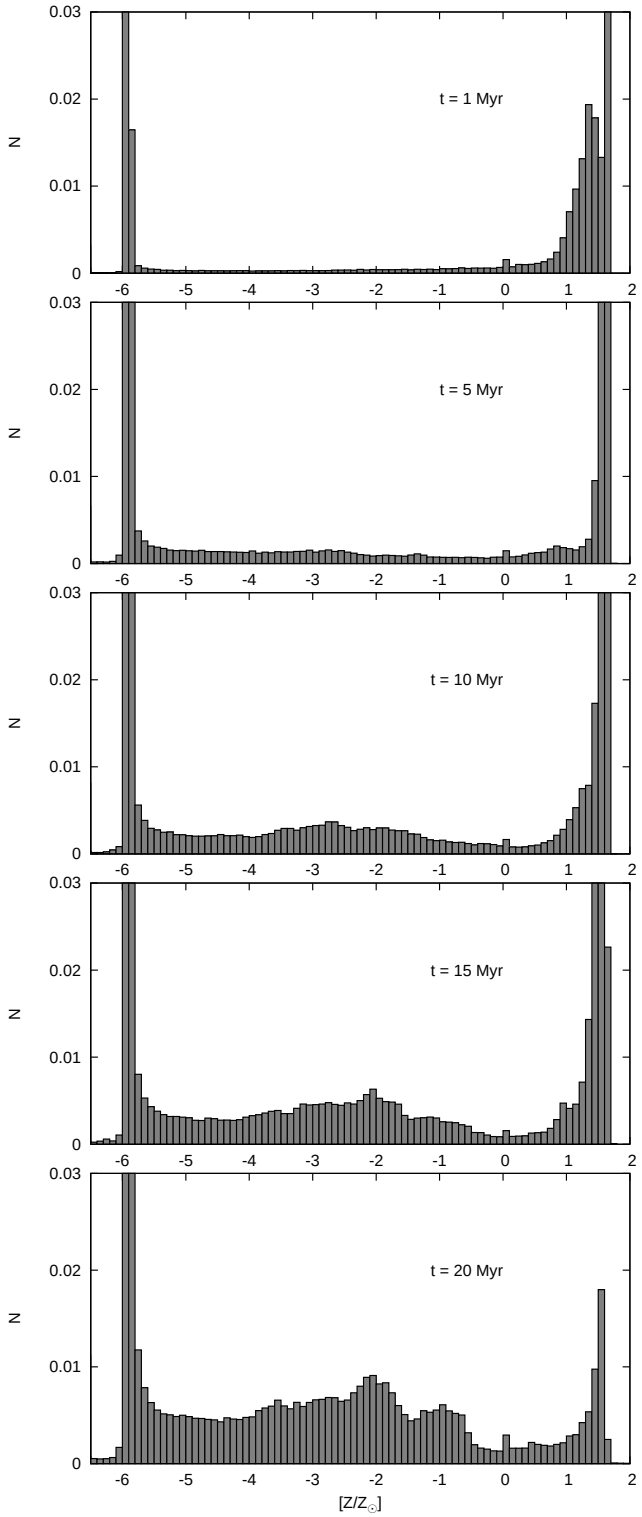

Figure 7: Distribution of the number of computation cells over gas metallicity $N(Z)$, normalized to the total number of computation cells, for a SN explosion with energy 10^{52} erg and initial stellar mass 140 $M_\odot$ at times 1, 5, 10, 15, and 20 Myr (from top to bottom).

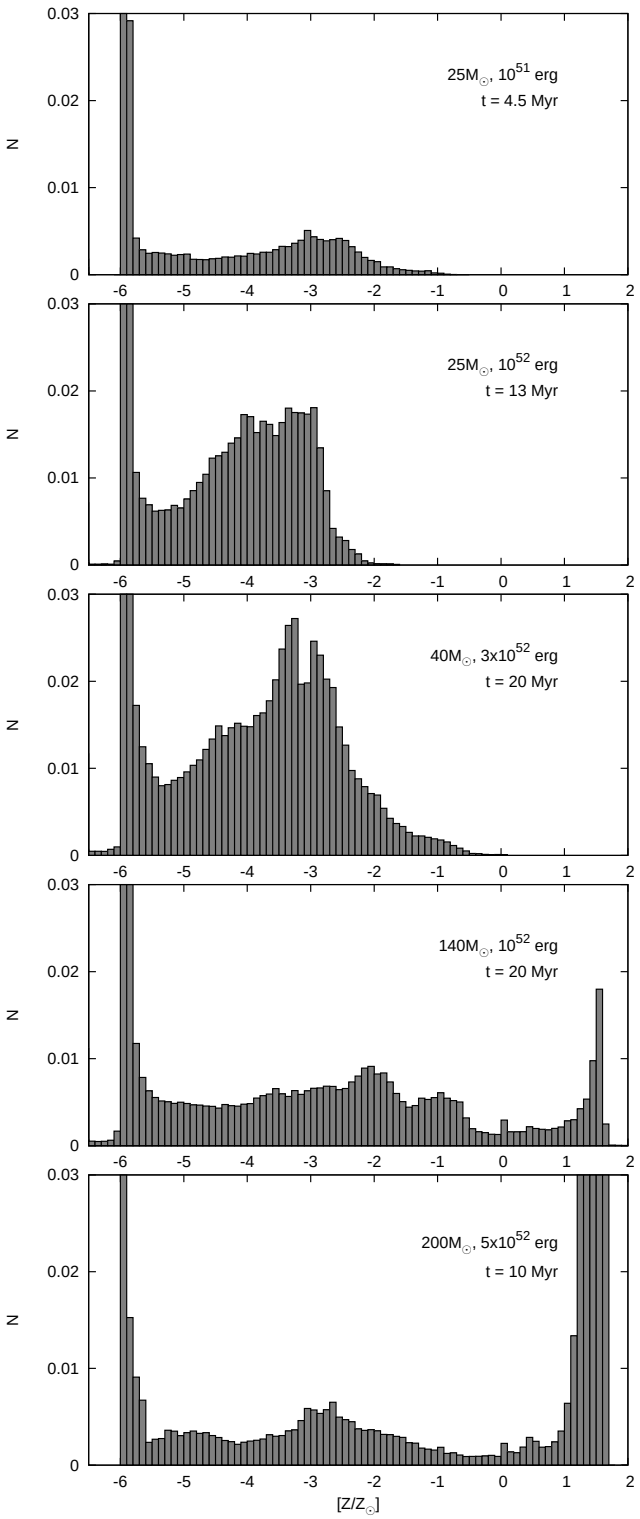

Figure 8: Distribution of the number of computation cells over the gas metallicity $N(Z)$, normalized to the total number of computation cells, for a SN explosion with energy E and initial mass M.

gas with themaximummetallicity remains up to the final time, implying incomplete mixing of the cavity gas. The redistribution of heavy elements proceeds non-uniformly. A dip in the distribution at $Z \sim Z_\odot$ and a growth in the number of cells with metallicity $\sim 10^{-2}\ Z_\odot$ can be seen. The number of cells with low metallicities $(10^{-5} - 10^{-3})\ Z_\odot$ also increases. The gas with such metallicities is primarily concentrated in fragments of the envelope that have reached the periphery of the protogalaxy, $r \gtrsim 0.5 r_v$. The temperature of this gas is below 1000 K, and its number density is above 1 cm^{-3}. These fragments also contain a large amount ofmolecular hydrogen, so that they are able to cool even further. Their properties will be considered in more detail below.

The gas in the collapsing SN envelopes mixes with the high-metallicity gas of the cavity due to the action of numerous shocks and circum-sonic waves that form during the motion of converging flows of gas in the central region of the protogalaxy (see the preceeding section). Therefore, the region of gas with initially high metallicity disappears, but the metallicity of the gas becomes appreciably higher as the distribution of heavy elements in the protogalaxy becomes more uniform (perfectly uniform in the case of total mixing): $Z \sim M_{met}/M_{gas}$, where M_{met} and M_{gas} are the masses of metals ejected by the SN (Table) and the mass of gas in the protogalaxy. This is clearly visible in Fig. 8, which presents the distribution of the number of computation cells over the gas metallicity $N(Z)$ normalized to the total number of computation cells for a SN explosion with energy E and initial mass M. In fully collapsed SN envelopes (top three histograms), no gas with the metallicity of the ejected gas remains at the end of the computations. The largest numbers are displayed by cells with metallicities in the interval $(10^{-4} - 10^{-2})\ Z_\odot$ or with the background metallicity $10^{-6}\ Z_\odot$. The partially collapsed SN envelope with $M = 140\ M_\odot$ shows the presence of the high-metallicity gas of the cavity (see the fourth histogram from the top in Figs. 8 and 7). In an expanding SN remnant with $M = 200\ M_\odot$, we can distinguish the background gas with $Z = 10^{-6}\ Z_\odot$, hot cavity gas in which $Z \gtrsim 10\ Z_\odot$, and gas in enriched envelope fragments and thread-like structures (Fig. 3) with metallicities $Z \sim 10^{-2}\ Z_\odot$.

Although the distribution of the number of cells over metallicity correctly reproduces the variations in the character of the spatial distribution of metals with time, it gives an incorrect impression of the filling factors in the regions with various metallicities, and consequently of the masses of metals contained in these regions. This is associated with the cylindrical geometry of our model: the cells located a distance r from the cylinder axis correspond to proportionally larger volumes. An example of the dependence of the mass and volume of the gas with metallicities above a specified level and in metallicity intervals after a SN explosion with initial mass $140\ M_\odot$ and energy 10^{52} erg was shown in Fig. 4, and this dependence was described in the previous section. Here, we list the main properties of this dependence characteristic for collapsing SN envelopes, rather than presenting figures for all our models. First, the mass of enriched gas with metallicities $[Z] > -5$ grows with time, and approaches a saturation value. Second, the gas in the central region of the protogalaxy continues to have metallicities $[Z] > -2$, and the gas in fragments is not enriched above $[Z] \sim -2$. Third, the volume occupied by high-metallicity gas ($[Z] > 0$) at the onset of the evolution of the SN envelope grows, then decreases, corresponding to the initial expansion and subsequent compression of the hot cavity. The mass of such gas remains nearly constant with time, and falls off after the onset of mixing of the cavity gas and the incident gas in the collapsing envelope. Finally, the largest amount of gas by mass and volume is that with intermediate metallicities $-3.5 < [Z] < -2$.

Figure 9 presents the "metallicity-density" diagram for all our models. A typical feature of the distibutions is a incomplete mixing with an exceptionally high spread of metallicities in the whole region covered by the remnant: $-5 < [\mathrm{Z}] < +1$. It is worth stressing that incomplete mixing takes place not only in first protogalaxies, but in the Galactic interstellar and intergalactiic media as well [43-45]. The isolines show the mass of gas with the indicated density and

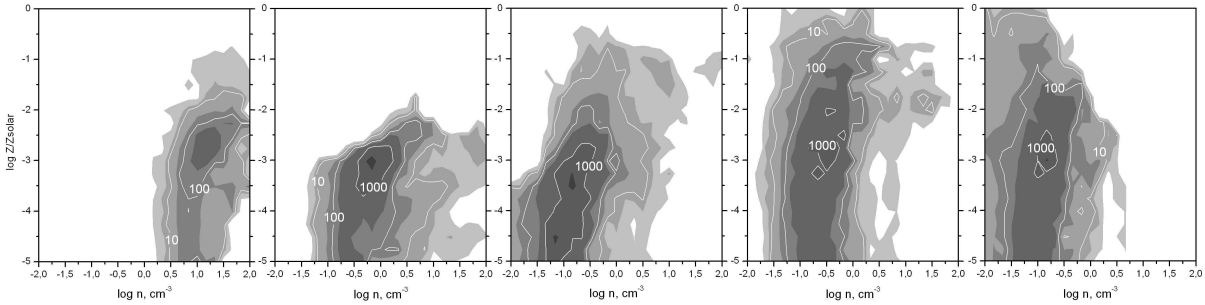

Figure 9: The "metallicity-density" diagram in gas at final time after SN explosion with the energy E and the progenitor mass M (left to right): $t = 4.4$ Myr for a star with $M = 25\ M_\odot$ and a SN energy $E = 10^{51}$ erg, $t = 13$ Myr for $M = 25\ M_\odot$ and $E = 10^{52}$ erg, $t = 20$ Myr for $E = 40\ M_\odot$, $E = 3 \times 10^{52}$ erg, $t = 20$ Myr for $M = 140\ M_\odot$, $E = 10^{52}$ erg, $t = 16$ Myr for $M = 200\ M_\odot$ and $E = 5 \times 10^{52}$ erg. The isolines show those cells with given density and metallicity where the mass content equals the indicated value.

metallicity. It is readily seen that independent on model (e.g. pre-supernova density profiles, SN energy, final time etc.) the peak mass ($M \sim 100 - 1000 M_\odot$) is located at metallicities $-3.5 < [Z] < -2$. This circumstance allows us to conclude that incomplete mixing of metals in first SN remnants provide metallicities $-3.5 < [\mathrm{Z}] < -2$ typical for the old stellar population of the Milky Way halo. However, because the gas mass in the range $[Z] < -3.5$ drops very fast this incomplete mixing process cannot explain metallicities of extremely metal-poor stars which are typically below $[Z] < -3.5$ [46-51] (see in particular [52]). This requiers a separate study.

Figure 3 shows that the SN envelope is strongly disrupted, and its fragments contain cool, denise gas enriched in metals. These fragments are $\sim 1-10$ pc in size, and have densities a factor of ten or more higher and temperatures a similar factor lower than the surrounding regions. The further from the center of the protogalaxy, the lower the density of the gas in the fragments. Thus, the fragments remaining after the disruption of the envelope of a SN with initial mass 140 $M_\odot$ and energy 10^{52} erg turn out to be less dense than in the case of a SN with $M = 25\ M_\odot$ and $E = 10^{51}$ erg. This can easily be explained by the value of the surrounding gas density at the onset of the disruption of the SN envelope: the lower the explosion energy, the smaller the size of the envelope when it begins to disrupt. The fragments possess primarily supersonic velocities. Gas densifications associated with the propagation of the shock front can be noted around the fragments at the periphery of the protogalaxy. The fragments moving toward the center also have supersonic velocities of the order of several km/s. The characteristic time for the disruption of such fragments when they are ripped apart by the Kelvin-Helmholtz instability is several million years. On the other hand, the fairly high metallicity, $[Z] \sim -3$, and H_2 number density $\sim 2 \times 10^{-3}$, of the fragments facilitate rapid cooling of the gas over a time scale shorter than those for their disruption or destruction. However, a substantial number of fragments in the central region are disrupted by collisions, hindering efficient cooling and the formation of protostellar condensations.

The identification of distinct fragments with densities higher than a specified level (using the method described in [52, 60]) showed that the masses of these fragments are smaller than the Jeans mass. A central, cool, denise fragment gradually forms in collapsing SN envelopes, which contain a larger amount of heavy elements than similar fragments at the protogalaxy periphery. The mass of this fragment grows due to the infalling gas, which rapidly cools due to energy losses in lines of heavy elements. We ceased our computations when a gravitational-compression regime was established in the central region of the protogalaxy, i.e., when the gas density reached $n \sim 10^6$ cm^{-3} (the reasons for this are indicated above). By this time, the mass of the central

fragment with a density above 10^{-3} cm^{-3} reaches $\sim 70\ M_\odot \sim 1/4 M_J$ for a SN with $M = 25\ M_\odot$ and $E = 10^{51}$ erg, and will probably continue to grow further. The mass of this fragment is $\sim 2 \times 10^3\ M_\odot \gtrsim 100 M_J$ for a SN with $M = 25\ M_\odot$ and $E = 10^{51}$ erg, as well as a SN with $M = 40_\odot$ and $E = 3 \times 10^{52}$ erg. The mean density, temperature, and metallicity of the gas in the fragment are approximately $\sim 10^5$ cm^{-3}, ~ 40 K, and $\sim 0.01\ Z_\odot$. It is obvious that the birth of a group of stars with various masses (including some with masses comparable to the solar mass) will subsequently be possible in this region of gas, whose lifetimes will be several billions of years. These could live to the current epoch and be observed in the Galaxy. Moreover, the birth of stars with high masses $\gtrsim 10 M_\odot$ is probable, whose ultraviolet radiation and explosions as SN could faciliate subsequent mixing of heavy elements. Finally, in the case $M = 140\ M_\odot$ and $E = 10^{52}$ erg, the mass of the central fragment turns out to be substantially lower than the corresponding Jeans mass, although the number density at the center reaches $n \sim 10^6$ cm^{-3}. It is possible that such a central fragment could subsequently become gravitationally bound.

5 Discussion

Some consequences of SN explosions (such as the formation of low-mass galaxies with virtually no gas) and possible problems with our computations (in particular, failure to take into account CO and OH molecules) are discussed above. All the computations for which results are presented above assumed that a single massive star was born in the initial phase of the protogalaxy, due to inefficiency of fragmentation in that stage, as was manifest in the numerical computations of [6]. However, the conditions for the formation of a large number of protostellar fragments could well arise in rotating protogalaxies or strongly turbulent gas [7–10]. Consequently, numerous SN explosions are, in principle, possible in the first protogalaxies. Of course, the initial surrounding gas would be ionized by radiation from such a cluster of first-generation stars, whose masses would likely be fairly high due to the low opacity of the primordial gas [3]. Therefore, the gas in, and probably beyond, the protogalaxy will be ionized, although this depends on the mass function of these first stars. Here, we should bear in mind that such a cluster will not contain many first stars (the mass of cool gas in a low-mass protogalaxy cannot be high), so that the masses of stars in the cluster will be distributed randomly over a wide interval, e.g., $M \sim 10 - 1000\ M_\odot$. It seems unlikely that most of these will be stars with masses of 140–260 $M_\odot$, capable of exploding as high-energy supernovae. Since some of these stars could form black holes (40–140 $M_\odot$), they could participate only in the formation of the ionization zone. The few stars that explode as supernovae will probably explode nearly simultaneously, forming an envelope equivalent to that for a single supernova with the same total power.

Let us suppose that the stars in such a cluster were born approximately simultaneously. In this case, the envelope of a SN explosion of a star with mass 140 $M_\odot$ and energy 10^{52} erg will still be expanding $\sim$5-6 Myr after the explosion (Fig. 1), so that a star with mass 25 $M_\odot$ (with a lifetime of 6.5 Myr) could explode before the envelope of the preceding SN cools and collapses. In this case, the shocks from the second and preceding supernovae will propagate through highly enriched gas (or capture this gas, if the parent stars are appreciably separated in space), stimulating mixing of the gas during the collision at the inner side of the first envelope.

If the birth of stars in the cluster takes place over an appreciable time, the envelope from the first supernova could have time to potentially cool and fragment. The influence of the ionization fronts from other stars and the subsequent action of the shock front on other supernovae could then both disrupt fragments in the first envelope and stimulate their compression, i.e., stimulate star formation. The efficiency of mixing of metals will obviously increase in this case due to the additional energy supplied (see the Introduction). Taking into account our comments about mixing and the results presented in the previous sections, we conclude that, after the explosions of the first supernovae, it is probably difficult to detect a clear relationship between

the metallicities of stars and the generation in which they were born. Thus, both stars with metallicities close to the solar value (incomplete mixing) and metal-poor stars (complete mixing) could be born in gas enriched by the first stars.

Recently, the evolution of the first stars with rotation has been considered [82]. The winds from such stars could be fairly powerful, and could contain a significant amount of metals in later stages of the stars lifetime [82]. Thus, rotating stars could exert a significant chemical effect on the surrounding gas, even before their explosion as supernovae. The efficiency of this effect depends on the mass of metals in the stellar wind and the velocities of gas outflows from the stellar surfaces [83].

Finally, dust particles can form in SN remnants [8487], which can play a appreciable role in star formation. First, dust particles substantially increase the opacity of a medium, facilitating efficient fragmentation and a transition to the birth of low-mass stars [88], compared to the case of gas without dust [34-37]. Second, the formation of molecular hydrogen is appreciably enhanced in the presence of dust [89], likewise leading to more efficient cooling of the gas and facilitating the birth of lower-mass stars. However, the transport and mixing of dust could differ substantially from the transport of gas particles, since dust is appreciably heavier and has appreciably lower charge-to-mass ratios than ions; in addition, dust will be disrupted behind shock fronts [90], and can grow in cool, dense clouds [91]. Therefore, the questions of the transport of dust, and also of its formation in SN, remain open [84, 87, 92], and requires a separate discussion.

6 Conclusions

We have considered the dynamical, thermal, and chemical evolution of gas in supernova envelopes from first stars with masses$M_* \sim 25-200\ M_\odot$ in protogalaxies with mass $M \sim 10^7\ M_\odot$ at redshifts $z = 12$, and analyzed the efficiency of mixing of heavy elements produced in these first stars. The SN explosions occur inside the ionization zone formed by the star. In particular, we have shown the following.

1. During SN explosions with high energies ($E \gtrsim 5 \times 10^{52}$ erg), an appreciable amount of gas can be ejected from the protogalaxy, but nearly all the metals produced remain inside the galaxy. The hot, enriched gas occupies a central volume with a radius up to half the virial radius for a protogalaxy with $M \sim 10^7\ M_\odot$; the cooling time in this hot gas is of order several million years – comparable to or longer than the time for the loss of a substantial fraction of the gas mass (more than 50%). Thus, protogalaxies in which high energy SN explosions occur may be transformed into "dark" objects with virtually no gas.

2. During SN explosions with lower energies ($E \lesssim 3 \times 10^{52}$ erg), essentially no gas and heavy elements are lost from a protogalaxy with $M \sim 10^7\ M_\odot$. During the first 1-3 Myr, gas and heavy elements are actively carried from the central region of the protogalaxy: up to 90% of the mass of metals is carried beyond a radius of 0.05 times the virial radius during a SN explosion with an initial mass of 25 $M_\odot$ and energy $E = 10^{51}$ erg, and beyond a radius of 0.1 times the virial radius during a SN explosion with an initial mass of 40 $M_\odot$ and energy $E = 3 \times 10^{52}$ erg or a SN explosion with an initial mass of 140 $M_\odot$ and energy $E = 10^{52}$ erg. However, during the subsequent evolution, an appreciable fraction of the mass of metals returns to the center as the hot cavity is cooled and the envelope collapses.

3. High-energy supernovae ($E \gtrsim 5 \times 10^{52}$ erg) are characterized by a low efficiency of mixing of metals. Heavy elements are located in a small volume in the disrupted envelope (compared to the entire volume of the envelope), and the bulk of the metals remain inside the hot, rarified cavity.

4. The efficiency of mixing of heavy elements for lower-energy supernovae ($E \lesssim 3 \times 10^{52}$ erg) is appreciably higher than for SN with energies $E \gtrsim 5 \times 10^{52}$ erg due to the disruption of the hot cavity during the collapse of the SN envelope. However, a clear distinction between enriched and unenriched (primordial) regions is observed; i.e., the mixing remains incomplete.

5. During the collapse of the SN envlope, the hot, metal-rich gas of the cavity mixes with the cool, primordial (metal-poor) gas of the envelope. Therefore, the metallicity is appreciably higher in the central region of the protogalaxy ($[Z] \sim -1$ to 0) than in peripheral regions ($[Z] \sim -2$ to -4). The bulk of the enriched gas has metallicities $[Z] \sim -3.5$ to -2.5.

6. The enriched regions in the SN envelope are mainly characterized by fairly high metallicities $[Z] \gtrsim -3$ (higher than the critical value $[Z]_{cr} \sim -3.5$) and high H_2 abundances ($x(H_2) \gtrsim 10^{-3}$). The densities of such regions turn out to be substantially higher, and their temperatures substantially lower, than the mean values for the surrounding gas; however, their masses are appreciably lower than the Jeans mass, except in the central region of the protogalaxy. The ambient enriched gas accretes efficiently into the central region, and the birth of stars with metallicities close to those characteristic of modern stars in the Galaxy is very probable in this region.

7 Acknowledgements

This work was supported by the Russian Foundation for Basic Research (projects 09-02-00933, 11-02-00621, 11-02-01332, 11-02-90701, 11-02-97124, 12-02-90800), the Dinasty Noncommercial Foundation, the Austrian Science Foundation (FWF; grant M 1255-N16), and the Ministry of Education and Science of the Russian Federation (state contract P- 685). The computations were carried out on clusters of the Computational Center of the Southern Federal University.

References

[1] M. Tegmark, J. Silk, M.J. Rees, A. Blanchard, T. Abel, F. Palla, Astrophys. J. **474**, 1 (1997)

[2] Yu.A. Shchekinov and E.O. Vasiliev, Monthly Notices Roy. Astronom. Soc. **368**, 454 (2006)

[3] S.C.O. Glover, Space Sci. Rev. **117** 445 (2005)

[4] K. Omukai and F. Palla, Astrophys. J. **589** 677 (2003)

[5] D. Schaerer, Astron. and Astrophys **382**, 28 (2002)

[6] T. Abel, G.L. Bryan, and M.L. Norman, Sci, **295**, 93 (2002)

[7] P.C. Clark, S.C.O. Glover, R.S. Klessen, Astrophys. J. **672**, 757 (2008)

[8] A. Stacy, T.H. Greif, V. Bromm, Monthly Notices Roy. Astronom. Soc. **403**, 45 (2010)

[9] P.C. Clark, S.C.O. Glover, R.S. Klessen, V. Bromm, Astrophys. J. **727**, 110 (2011)

[10] E.O. Vasiliev, E.I. Vorobyov, and Yu.A. Shchekinov, Astron. Rep. **54**, 890 (2010)

[11] D. Whalen, T. Abel, M.L. Norman, Astrophys. J. **610**, 14 (2004)

[12] M.A. Alvarez, V. Bromm, P.R. Shapiro, Astrophys. J. **639**, 621 (2006)

[13] B. W. O'Shea, T. Abel, D. Whalen, M.L. Norman, Astrophys. J. Lett. **628**, 5 (2005)

[14] T. Abel, J.H. Wise, G.L. Bryan, Astrophys. J. Lett. **659**, 87 (2007).

[15] T. Kitayama, N. Yoshida, H. Susa, M. Umemura, Astrophys. J. **613**, 631 (2004)

[16] A. Mesinger, G.L. Bryan, Z. Haiman, Monthly Notices Roy. Astronom. Soc. **399**, 1650 (2009)

[17] D. Whalen, and M.L. Norman, Astrophys. J. **673**, 664 (2008)

[18] E.O. Vasiliev, E.I. Vorobyov, A.O. Razoumov, and Yu.A. Shchekinov, Astron. Rep. **56**, 564 (2012)

[19] V. Bromm, N. Yoshida, L. Hernquist, Astrophys. J. Lett. **596**, 135 (2003)

[20] T.H. Greif, J.L. Johnson, V. Bromm, R.S. Klessen, Astrophys. J. **670**, 1

[21] T. Nagakura, T. Hosokawa, K. Omukai, Monthly Notices Roy. Astronom. Soc. **399**, 2183 (2009)

[22] M. Trenti and M. Stiavelli, Astrophys. J. **694**, 879 (2009)

[23] T.H. Greif, S.C.O. Glover, V. Bromm, R.S. Klessen, Astrophys. J. **716**, 510 (2010)

[24] J.H. Wise and T. Abel, Astrophys. J. **685**, 40 (2008)

[25] J.H. Wise, M.J. Turk, M.L. Norman, T. Abel, Astrophys. J. **745**, 50 (2012)

[26] U. Maio, S. Khochfar, J.L. Johnson, B. Ciardi, Monthly Notices Roy. Astronom. Soc. **414**, 1145 (2011)

[27] A. Heger and S. Woosley, Astrophys. J. **567**, 532 (2002)

[28] C.C. Joggerst, A. Almgren, J. Bell, A. Heger, D. Whalen, S.E. Woosley, Astrophys. J. **709**, 11 (2010)

[29] C.C. Joggerst and D. Whalen, Astrophys. J. **728**, 129 (2011)

[30] T. Kitayama and N. Yoshida, Astrophys. J. **630**, 675 (2005)

[31] D. Whalen, B. van Veelen, B.W. O'Shea, M.L. Norman, Astrophys. J. **682**, 49 (2008)

[32] P. Madau, A. Ferrara, and M. Rees, Astrophys. J. **555**, 92 (2001)

[33] A. Ferrara, M. Pettini, and Yu. A. Shchekinov, Monthly Notices Roy. Astronom. Soc. **319**, 539 (2000)

[34] V. Bromm, A. Ferrara, P.S. Coppi, R.B. Larson, Monthly Notices Roy. Astronom. Soc. **328**, 969 (2001)

[35] V. Bromm and A. Loeb, Natur. **425**, 812 (2003)

[36] F. Santoro and J.M. Shull, Astrophys. J. **643**, 26 (2006)

[37] K. Omukai, T. Tsuribe, R. Schneider, A. Ferrara, Astrophys. J. **626**, 627 (2005)

[38] M.L. Norman, AIP Conf. Proc. **1294**, 17 (2010)

[39] U. Maio, B. Ciardi, K. Dolag, L. Tornatore, S. Khochfar, Monthly Notices Roy. Astronom. Soc. **407**, 1003 (2010)

[40] J. Mackey, V. Bromm, L. Hernquist, Astrophys. J. **586**, 1 (2003)

[41] A.A. Kabanov and B.M. Shustov, Astron. Rep. **55**, 784 (2011)

[42] T. Karlsson, V. Bromm, J. Bland-Hawthorn, Rev. Mod. Phys., accepted, arXiv1101.4024 (2011)

[43] M.A. de Avillez, M.-M. Mac Low, Astrophys. J. **581**, 1047 (2002)

[44] S.Yu. Dedikov and Yu.A. Shchekinov, Astron. Rep. **48**, 9 (2004)

[45] E.O. Vasiliev, S.Yu. Dedikov, and Yu.A. Shchekinov, Astrophys. Bull. **64**, 317 (2009).

[46] T. Beers, G. Preston, and S. Shectman, Astronom. J. **103**, 1987 (1992)

[47] N. Christlieb, M.S. Bessel, T.C. Beers, et al., Natur. **419**, 904 (2002)

[48] J.E. Norris, N. Christlieb, A.J. Korn, K. Eriksson, M.S. Bessell *et al.* Astrophys. J. **670**, 774 (2007)

[49] A. Frebel, R. Collet, K. Eriksson, N. Christlieb, W. Aoki, Astrophys. J. **684**, 588 (2008)

[50] M.S. Bessell, N. Christlieb, B. Gustafsson, Astrophys. J. Lett. **612**, 61 (2004)

[51] A. Frebel, N. Christlieb, J.E. Norris, W. Aoki, M. Asplund, Astrophys. J. Lett. **638**, 17 (2006)

[52] E. Caffau, P. Bonifacio, P. Fran cois, L. Sbordone, L. Monaco *et al.* Natur. **477**, 67 (2011)

[53] E.T. Vishniac, Astrophys. J. **274**, 152 (1983)

[54] F. Hoyle, in Problems of Cosmical Aerodynamics, ed. J. M. Burgers and H. C. van de Hulst (Dayton: Centeral Air Documents Office), 195 (1949)

[55] P.J.E. Peebles, Astrophys. J. **155**, 393 (1969)

[56] A. G. Doroshkevich, Astrofizika **6**, 581 (1970)

[57] A.G. Doroshkevich, Astrophys. Lett. **14**, 11 (1973)

[58] J.H. Wise and T. Abel, Astrophys. J. **665**, 899 (2007)

[59] D.N. Spergel, R. Bean, O. Doré, et. al., Astrophys. J. Suppl. Ser. **170**, 377 (2007)

[60] E.O. Vasiliev, E.I. Vorobyov, Yu.A. Shchekinov, Astron. and Astrophys. **489**, 505 (2008)

[61] S.W. Stahler, F.H. Shu, R.E. Taam, Astrophys. J. **241**, 637 (1980)

[62] B. Ciardi and A. Ferrara, Space Sci. Rev. **116**, 625 (2005)

[63] S.A. Woosley and T.A. Weaver, Astrophys. J. Sup. Ser. **101**, 181 (1995)

[64] M.L. Norman, J.R. Wilson, R. Barton, Astrophys. J. **239**, 968 (1980)

[65] P. Collela and P.R. Woodward J. Comp. Phys. **54**, 174 (1984)

[66] E.I. Vorobyov, U. Klein, Yu.A. Shchekinov, J. Ott, Astron. and Astrophys. **413**, 939 (2004)

[67] P.R. Shapiro and H. Kang, Astrophys. J. **318**, 32 (1987)

[68] T. Abel, P. Anninos, Yu. Zhang, M.L. Norman, New Astron. **2**, 181 (1997)

[69] D. Galli, and F. Palla, Astron. and Astropys. **335**, 403 (1998)

[70] W.H. Press, S.A. Teukolsky, W.T. Vetterling, B.P. Flannery, B. P., Numerical Recipes in FORTRAN, 2nd ed., Cambridge: Cambridge Univ. Press (1992)

[71] R. Cen, Astrophys. J. Suppl. Ser. **78**, 341 (1992)

[72] D. Flower, Mon. Not. Roy. Astron. Soc. **318**, 875 (2000)

[73] A. Lipovka, R. Núñez-López, V. Avila-Reese, Mon. Not. Roy. Astron. Soc. **361**, 850 (2005)

[74] E.O. Vasiliev, Mon. Not. Roy. Astron. Soc. **414**, 3145 (2011)

[75] D.A. Varshalovich and V.K. Khersonskii, Sov. Astron. Lett. **2**, 227 (1976)

[76] D. Puy, G. Alecian, J. Le Bourlot, J. Leorat, G. Pineau Des Forets, Astron. and Astropys. **267**, 337 (1993)

[77] D.A. Varshalovich, V.K. Khersonskii, and R.A. Syunyaev, Astrofizika **17**, 487 (1981)

[78] J.S. Bullock, in XX Canary Islands Winter School of Astrophysics on Local Group Cosmology, Ed. D. Martínez-Delgado, , arXiv:1009.4505

[79] R.S. de Souza, L.F.S. Rodrigues, E.E.O. Ishida, R. Opher, Monthly Notices Roy. Astronom. Soc. **415**, 2969 (2011)

[80] G. Ogiya and M. Mori, Astrophys. J. Lett. **736**, 2 (2011)

[81] F. Governato, A. Zolotov, A. Pontzen, C. Christensen, S.H. Oh, *et al.* Monthly Notices Roy. Astronom. Soc., , arXiv1202.0554G

[82] S. Ekstroḿ, G. Meynet, C. Chiappini, R. Hirschi, A. Maeder, Astron. Astrophys. **489**, 685 (2008)

[83] A. Stacy, V. Bromm, A. Loeb, Mon. Not. Roy. Astron. Soc. **413**, 543 (2011)

[84] B.E.K. Sugerman, B. Ercolano, M.J. Barlow, et al., Sci. **313**, 196 (2006)

[85] A. Venkatesan, B.B. Nath and J.M. Shull, Astrophys. J. **640**, 31 (2006)

[86] N. Smith, J.M. Silverman, A.V. Filippenko, et al., Astron. J. **143**, 17 (2012)

[87] S. Bianchi, R. Schneider, R. Valiante, ASP Conf. Ser. **414**, 65 (2009)

[88] T. Tsuribe and K. Omukai, Astrophys. J. Lett. **642**, 61 (2006)

[89] D. Hollenbach and C.F. McKee, Astrophys. J. Suppl. Ser. **41**, 555 (1979)

[90] B.T. Draine and E.E. Salpeter, Astrophys. J. **231**, 77 (1979)

[91] B.T. Draine, in: *The Cold Universe: Saas-Fee Advenced Course 32*, A.W. Blain, F. Combes, B.T. Draine, D. Pfenniger and Y. Revaz, eds., Berlin: Springer-Ferlag, 2004, p. 213

[92] W.P.S. Meikle, S. Mattila, A. Pastorello, et al., Astrophys. J. **665**, 608 (2007)